

«Original»

## Nuclear Design Analysis of Wolsung-1 CANDU-PHW Nuclear Generating Station

Chang Hyun Chung, Keun Bae Oh and C.H. Kim

College of Engineering, Seoul National University

Yo Han Chang, Seong Yun Kim and Jin Soo Kim

Korea Atomic Energy Research Institute

(Received November 10, 1978)

### Abstract

A combination of computer codes such as LATREP, HWRAXAV and CITATION is utilized in an attempt to analyze the nuclear design characteristics of the CANDU-PHWR of the Wolsung Unit 1. The major nuclear properties to be computed are the lattice properties of CANDU fuel channel and the core channel power distribution. The computed results are compared with the PSR documentation for the Wolsung reactor. The observed discrepancies between our computations and the PSR values are discussed in terms of incomplete information on the description of the core configuration in the PSR and the different calculation methods.

### 요 약

전산 코드인 LATREP, HWRAXAV 및 CITATION 을 이용하여 CANDU-PHWR 인 월성 1호기의 핵설계 특성 해석을 시도하였다. 계산된 주요 핵 특성은 CANDU 핵 연료봉 집합체에 대한 격자상수와 로심내의 출력 분포이며 그 계산 결과는 월성 1호기의 예비 안전성 보고서와 비교되었다. 계산치와 예비안전성 보고서에 제시된 설계치 사이의 차이점에 관해서는 예비안전성 보고서의 로심 기술에 대한 불완전한 자료와 계산 방법이 서로 다르다는 관점에서 검토되었다.

### 1. Introduction

The Wolsung Unit 1 is the first CANDU-PHWR nuclear power plant in Korea. The Wolsung CANDU reactor, as its name bears, uses deuterium oxide (heavy water) as moderator and natural uranium dioxide as fuel. It is manufactured in Canada by Atomic Energy of Canada Limited (AECL) and has the design capacity of 2,180 MW thermal power or 620 MW equivalent electrical power.

The unit is currently under construction by the Korea Electric Company with target completion date of April 1982. Various safety features of the plant is documented in a sequence of the Preliminary Safety Reports<sup>1-3)</sup> (PSR) by AECL.

This paper is intended for analyzing nuclear design characteristics of the Wolsung Unit 1 reactor on the basis of core physics codes available to us at the present moment. The major nuclear characteristics to be analyzed are the multiplication properties of the fuel channels

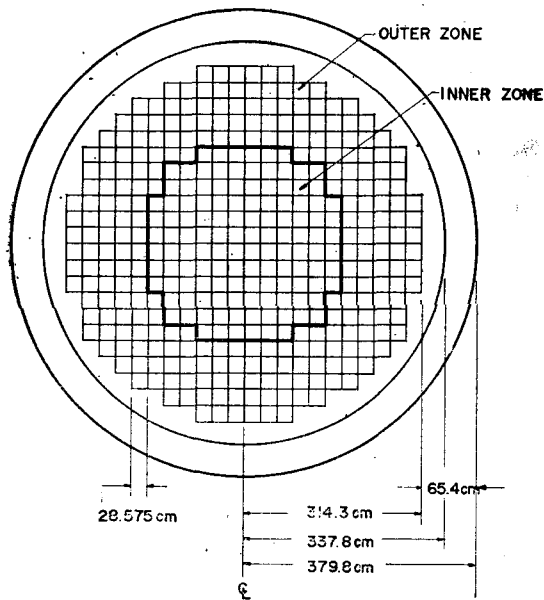


Fig. 1. Side View of the Wolsung PHWR Core

which consist of fuel bundle, pressure tube, calandria tube and moderator, and the core channel power distribution.

Three principal computer codes are adopted; LATREP<sup>4,5)</sup>, HWRAXAV<sup>6)</sup> and CITATION<sup>7)</sup>. The adoption of these codes is not generally recognized in the CANDU-reactor physics analysis, yet our computation results in a certain degree of satisfaction and discrepancies when compared with PSR values. The discrepancies between PSR and our computation are discussed in terms of uncertain PSR information with regard to the core description and calculator methods.

## 2. Description of CANDU-PHWR

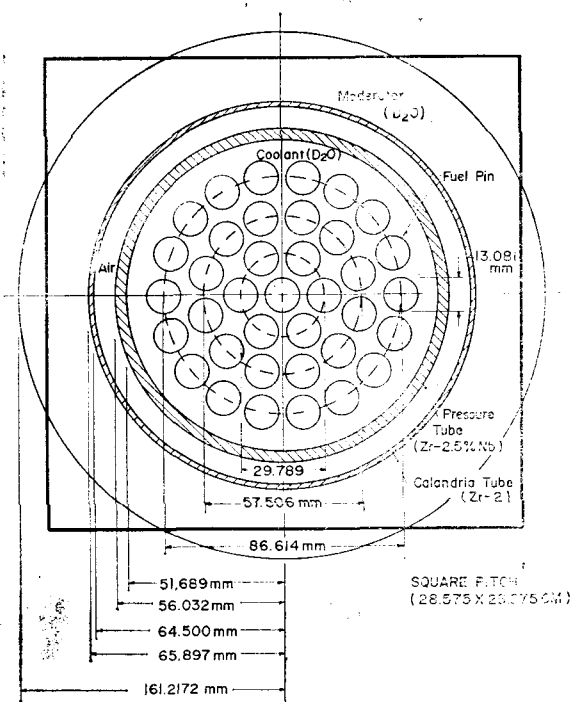
Description of CANDU-PHWR is well documented in PSR<sup>3)</sup>. Summarized in the following is a brief information that affects the lattice cell and core physics computations of Wolsung Unit 1.

CANDU-PHWR is composed of the reactor

core, the D<sub>2</sub>O reflector and the stainless steel calandria reactor vessel. The calandria which envelopes the fuel channels and contains heavy water moderator and reflector is a horizontal cylindrical vessel of 379.7 cm in radius and 606 cm in extrapolated length. Fig. 1 depicts a skeleton diagram of the reactor which is viewed from the side of the reactor. The detailed geometrical information is also given in it.

Reactor core is nearly cylindrical, 594.4 cm in length and 314.3 cm in equivalent diameter. It is made up of 380 calandria tubes or fuel channels which pass from end to end through calandria. The fuel channels are arranged on

(A) Horizontal View



(B) Axial Arrangement of Fuel Channel

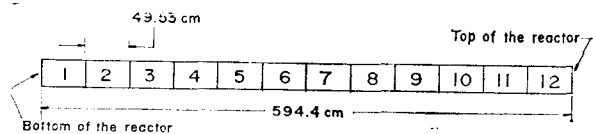


Fig. 2. Fuel Channel Dimension

**Table 1. Lattice Cell Data**

|  |                             |
|--|-----------------------------|
| Fuel   | 37 elements UO <sub>2</sub> |
| Element Outside Diameter                       | 13.081 mm                   |
| Air Gap Thickness                              | 0.0455 mm                   |
| Average Clad Wall Thickness                    | 0.419 mm                    |
| Pellet Outside Diameter                        | 12.154 mm                   |
| Stack Length (Bundle Length)                   | 480.31 mm                   |
| UO <sub>2</sub> Density                        | 10.6 g/cm <sup>3</sup>      |
| UO <sub>2</sub> Area                           | 42.926 cm <sup>2</sup>      |
| Coolant Area                                   | 34.211 cm <sup>2</sup>      |
| UO <sub>2</sub> Weight per Bundle              | 20.987 kg                   |
| Zircaloy Weight per Bundle                     | 2.2799 kg                   |
| Pressure Tube (Zr: 2.5% Nb)<br>Inside Diameter | 103.378 mm                  |
| Average Pressure Tube<br>Wall Thickness        | 4.343 mm                    |
| Calandria Tube (Zr-2) Inside<br>Diameter       | 129.0 mm                    |
| Average Calandria Tube<br>Wall Thickness       | 1.397 mm                    |
| Lattice Pitch                                  | 285.75 mm                   |
| Equivalent Channel Diameter                    | 322.4344 mm                 |

a regular square lattice with a center-to-center spacing of 28.575 cm. Each calandria tube contains a Zircaloy-2 pressure tube of 4.343 mm wall thickness and 103.38 mm inside diameter.

Inside the pressure tube resides 12 fuel bundles each of which comprises 37 fuel elements. D<sub>2</sub>O coolant is pumped through the fuel elements. The stagnant air gap between the calandria tube and pressure tube serves to insulate the hot heavy water coolant inside the pressure tube from the cold heavy water moderator surround-

ing the calandria tube.

Fig. 1 shows the initial core configuration which consists of two regions; depleted inner fuel region of 124 channels and undepleted outer fuel region of 256 channels. The inner fuel channels contain two depleted fuel bundles in which fuel (UO<sub>2</sub>) is depleted to 0.52 atom percent in U-235. Their axial location, however, is not known at the moment. Fig. 2 depicts the geometrical details on a fuel channel which forms a lattice cell together with surrounding heavy water. Table 1 summarizes dimensional information of the cell constituents required for the cell calculation.

### 3. Method of Nuclear Design Analysis

The nuclear physics parameters to be computed in this report are the lattice cell parameters, reactivity effects of temperature and the poison concentration and 2-dimensional core power distributions, etc. The numerical computations of these parameters are performed on the basis of three principal computer codes; LATREP, HWRAXAV and CITATION.

LATREP<sup>4,5)</sup> is a lattice cell code based on a multigroup collision probability method in which the fuelled cell calculation is carried out in 32 fast energy groups and one thermal group with thermal cut-off energy of 0.625 eV. The code has been extensively used for studying the lattice properties of CANDU-type reactor in

**Table 2. Lattice Cell Parameters for the Initial Undepleted Fresh Fuel Channels**

| Parameter    | Condition<br>Cold, Clean<br>Zero Power | Hot, Clean<br>Zero Power | Hot, Clean<br>Full Power | Hot, Full Power with<br>Equilibrium Poison |        |
|--------------|--|--------------------------|--------------------------|--|--------|
|              |  |                          |                          | LATREP                                     | PSR    |
| $\epsilon$   | 1.029707                               | 1.031529                 | 1.031542                 | 1.031527                                   | 1.026  |
| $\rho$       | 0.903086                               | 0.902081                 | 0.896286                 | 0.896286                                   | 0.9047 |
| $\eta$       | 1.319509                               | 1.309790                 | 1.301131                 | 1.244816                                   | 1.241  |
| $f$          | 0.932625                               | 0.934541                 | 0.933713                 | 0.935614                                   | 0.9358 |
| $k_{\infty}$ | 1.144358                               | 1.139009                 | 1.123228                 | 1.076786                                   | 1.078  |

Table 3. Temperature Specifications of Channel Components vs. Operating Condition

| Conditions<br>Temperature(°C) | Cold, Clean<br>Zero Power | Hot, Clean<br>Zero Power | Hot, Clean<br>Full Power | Hot, Full Power<br>with Equilibrium<br>Poison |
|-------------------------------|---------------------------|--------------------------|--------------------------|---|
| Fuel Pellet Temp. $T_f$       | 25°C                      | 290°C                    | 936°C                    | 936°C   |
| Clad Temp. $T_c$              | 25°C                      | 290°C                    | 339°C                    | 339°C   |
| Coolant Temp. $T_e$           | 25°C                      | 290°C                    | 290°C                    | 290°C   |
| Moderator Temp. $T_m$         | 25°C                      | 73°C                     | 73°C                     | 73°C  |

Table 4. Burnup Dependent Lattice Cell Parameters for Undepleted Fresh Fuel Bundle at HFP<sup>(1)</sup> Condition

| Burnup <sup>(2)</sup><br>Parameter | 0.0 n/kb <sup>(3)</sup> | 0.4 n/kb | 0.8 n/kb | 1.2 n/kb | 1.6 n/kb | 2.0 n/kb |
|------------------------------------|-------------------------|----------|----------|----------|----------|----------|
| $\epsilon$                         | 1.031532                | 1.031485 | 1.031464 | 1.031448 | 1.031428 | 1.031403 |
| $\rho$                             | 0.896336                | 0.896047 | 0.895850 | 0.895722 | 0.895654 | 0.895637 |
| $\eta$                             | 1.249914                | 1.245256 | 1.217855 | 1.182171 | 1.145688 | 1.111603 |
| $f$                                | 0.922746                | 0.927205 | 0.929802 | 0.931131 | 0.931889 | 0.932386 |
| $k_\infty$                         | 1.066388                | 1.067157 | 1.046347 | 1.016977 | 0.986301 | 0.957428 |
| $k_{eff}^{(3)}$                    | 1.036042                | 1.037818 | 1.018162 | 0.989867 | 0.960159 | 0.932144 |

(1) HFP: Hot Full Power (2) n/kb: neutrons per kilo-barn (3)  $B_g^2$  is taken as  $0.7618 \text{ m}^{-2}$

which fuel rods are arranged in the form of clusters inside the pressure tube. The accuracy of the code has been confirmed by comparing cell parameter measurements in ZED-II with the corresponding LATREP calculations<sup>(5)</sup>. In the present application this code is used for computing lattice cell parameters, cell burnup and equivalent homogenized diffusion theory parameters as the input of CITATION computer code.

HWRAVAV<sup>(6)</sup> is a perturbation theory code which provides a simple, consistent method of accounting for the axial variation in the lattice cell parameters of fuel channel. The code is primarily intended to convert the axially varying cell parameters for a given fuel channel into the equivalent values equal to the extrapolated core height and thus to prepare some of the basic input data for CITATION models of the three-dimensional reactor.

CITATION<sup>(7)</sup> is a few-group finite-difference diffusion theory code that can treat up to three

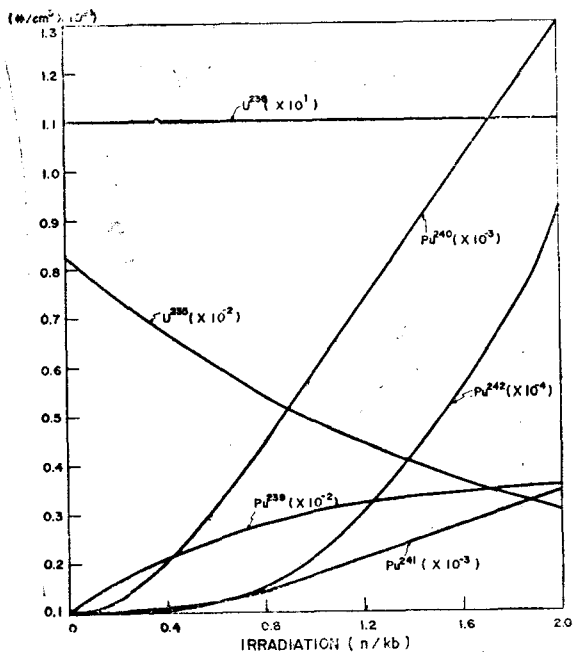


Fig. 3. Changes in Isotopic Composition versus Burnup

space dimensions with arbitrary group-to-group scattering. This code is used for determining 2-

**Table 5. Burnup Dependent Lattice Cell Parameters for Depleted Fresh Fuel Bundle at HFP<sup>1)</sup> Condition**

| Burnup<br>Parameter | 0.0 n/kb <sup>2)</sup> | 0.4 n/kb | 0.8 n/kb | 1.2 n/kb | 1.6 n/kb | 2.0 n/kb |
|---------------------|------------------------|----------|----------|----------|----------|----------|
| $\epsilon$          | 1.031446               | 1.031400 | 1.031387 | 1.031380 | 1.031370 | 1.031356 |
| $\rho$              | 0.895109               | 0.895004 | 0.894952 | 0.894941 | 0.894968 | 0.895027 |
| $\eta$              | 1.102449               | 1.144408 | 1.145086 | 1.127780 | 1.104778 | 1.081146 |
| $f$                 | 0.913527               | 0.920514 | 0.924654 | 0.926999 | 0.928496 | 0.929562 |
| $k_{\infty}$        | 0.929827               | 0.972441 | 0.977325 | 0.964976 | 0.946840 | 0.927701 |
| $k_{eff}^{3)}$      | 0.901503               | 0.944286 | 0.949901 | 0.938381 | 0.921043 | 0.902630 |

(1) HFP: Hot Full Power (2) n/kb: neutrons per kilo-barn (3)  $B_g^2$  is taken as  $0.7618 \text{ m}^{-2}$

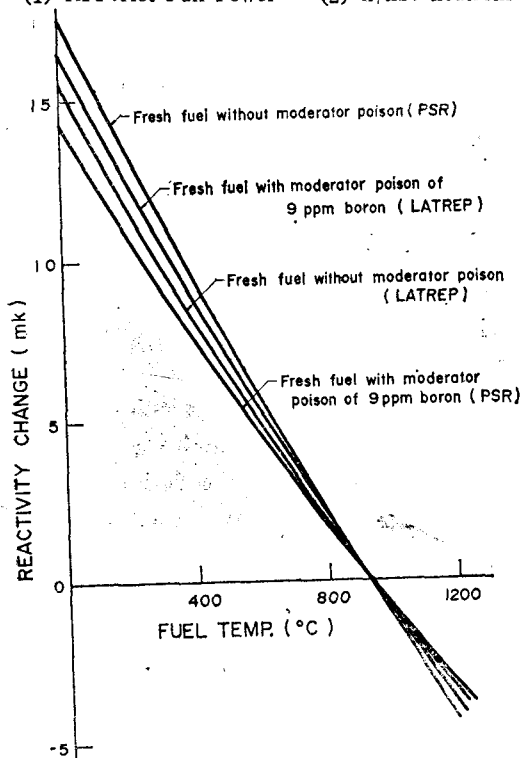


**Fig. 4. Effect of Fuel Temperature Change on  $k_{\infty}$**

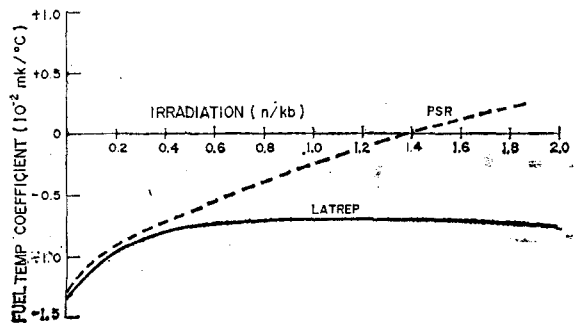


**Fig. 5. Variation of Fuel Temperature Coefficient of Reactivity with Fuel Irradiation**

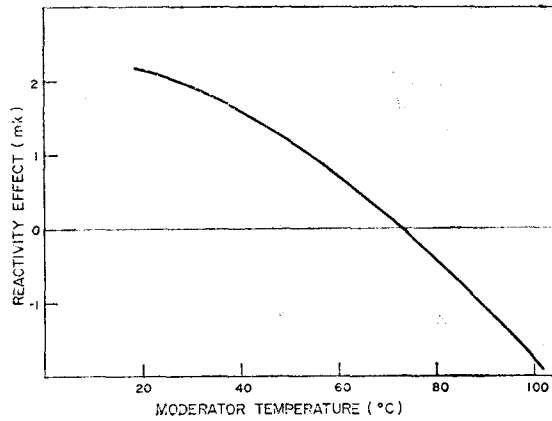


**Fig. 6. Reactivity Effects of the Moderator Temperature**

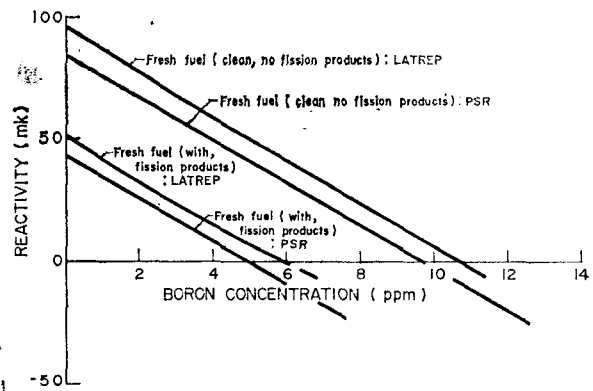


**Fig. 7. Variation of Reactivity with Moderator Poison Concentration**

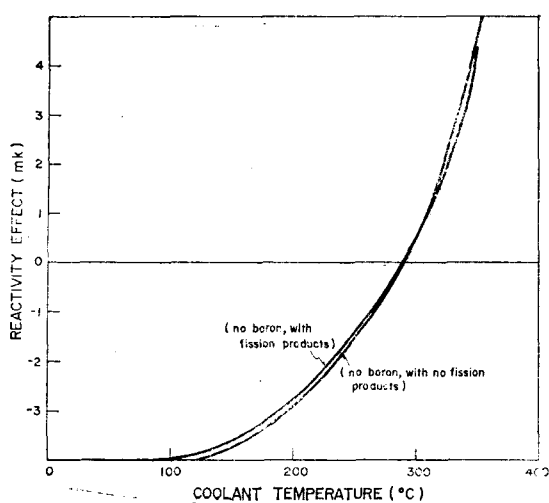


Fig. 8. Reactivity Effects of the Coolant Temperature

dimensional X-Y channel power distribution in terms of two-group representation of neutron flux.

#### 4. Results and Discussions

##### 4.1. Lattice Cell Parameters

The lattice cell parameters for the undepleted fresh fuel channels are calculated with LATREP<sup>4),5)</sup>.

The cell conditions of interest are (1) cold, zero power, (2) hot, zero power, (3) hot, full power and (4) hot, full power with equilibrium poison concentration.

The numerical results of LATREP for the undepleted fresh fuel channel are given in Table

2 along with the available PSR values. Just for the sake of clarity, the cell conditions are specified in terms of temperatures of cell components as shown in Table 3. Moderator is assumed boron-free and poison effects in condition (4) are taken into account using the equilibrium Xe-135 concentration of  $1.394 \times 10^{16}$  atoms/cm<sup>3</sup> and Sm-149 concentration of  $1.625 \times 10^{15}$  atoms/cm<sup>3</sup>.

The lattice cell parameters changes as fuel burnup proceeds and/or as the temperatures of cell components such as fuel rod, coolant and moderator deviate from respective reference value. Fig. 3 depicts the changes in isotopic composition of some important fuel nuclides versus burnup (in units of n/kb). The accompanying changes in lattice cell parameters for both depleted and undepleted fuel bundles are listed in Tables 4 and 5.

Fuel temperature affects the neutron multiplication through the Doppler broadening of U-238 and the spectrum change. As shown in Fig. 4, the overall effect of change in fuel temperature on the infinite multiplication factor is negative. Fuel burnup influences on the absolute value of fuel temperature reactivity coefficient. Both LATREP and PSR<sup>3)</sup> results for burnup dependent fuel temperature coefficient are shown in Fig. 5.

An increase in moderator temperature accompanies the spectrum hardening partly due to the increase in effective neutron temperature

Table 6. Equivalent Homogenized Two-Group Diffusion Theory Constants for Undepleted Fresh Fuel Bundle

| Parameter         | Condition | Cold, Clean Zero Power    | Hot, Clean Zero Power     | Hot, Clean Full Power     | Hot, Full Power with Equilibrium Poison |
|-------------------|-----------|---------------------------|---------------------------|---------------------------|---|
| $D_1$             |           | 1.280297                  | 1.315781                  | 1.303949                  | 1.303992                                |
| $D_2$             |           | 1.084772                  | 1.219619                  | 1.209147                  | 1.207045                                |
| $\Sigma_{a1}$     |           | $0.969235 \times 10^{-3}$ | $0.948518 \times 10^{-3}$ | $1.049285 \times 10^{-3}$ | $1.049285 \times 10^{-3}$               |
| $\Sigma_{a2}$     |           | $4.757211 \times 10^{-3}$ | $4.864226 \times 10^{-3}$ | $4.796183 \times 10^{-3}$ | $4.901861 \times 10^{-3}$               |
| $\Sigma_{r1}$     |           | $9.031741 \times 10^{-3}$ | $8.738245 \times 10^{-3}$ | $8.748788 \times 10^{-3}$ | $8.748790 \times 10^{-3}$               |
| $\nu \Sigma_{f2}$ |           | $6.028166 \times 10^{-3}$ | $6.141796 \times 10^{-3}$ | $6.039563 \times 10^{-3}$ | $5.915974 \times 10^{-3}$               |

**Table 7. Comparison of Two-Group Diffusion Theory Constants for HFP with Equilibrium Poison**

| Parameter                             | Region | PSR                      |                          |                          | LATREP                   |                           |                           |
|---------------------------------------|--------|--------------------------|--------------------------|--------------------------|--------------------------|---------------------------|---------------------------|
|                                       |        | Undepleted Fuel          | Depleted Fuel            | Reflector                | Undepleted Fuel          | Depleted Fuel             | Reflector                 |
| $D_1$ (cm)                            |        | 1.2739                   | 1.27396                  | 1.3171                   | 1.315774                 | 1.315937                  | 1.259745                  |
| $D_2$ (cm)                            |        | 0.94106                  | 0.93984                  | 0.87871                  | 1.217935                 | 1.211582                  | 0.886507                  |
| $\Sigma_{a1}$ (cm <sup>-1</sup> )     |        | $0.76604 \times 10^{-3}$ | $0.76746 \times 10^{-3}$ | 0                        | $0.10041 \times 10^{-2}$ | $0.101605 \times 10^{-2}$ | $0.109808 \times 10^{-2}$ |
| $\Sigma_{a2}$ (cm <sup>-1</sup> )     |        | $0.37312 \times 10^{-2}$ | $0.33621 \times 10^{-2}$ | $0.14299 \times 10^{-3}$ | $0.49488 \times 10^{-2}$ | $0.442594 \times 10^{-2}$ | $0.145163 \times 10^{-3}$ |
| $\nu \Sigma_{f2}$ (cm <sup>-1</sup> ) |        | $0.43716 \times 10^{-2}$ | $0.34312 \times 10^{-2}$ | 0                        | $0.58877 \times 10^{-2}$ | $0.459760 \times 10^{-2}$ | 0                         |
| $\Sigma_{r1}$ (cm <sup>-1</sup> )     |        | $0.73895 \times 10^{-2}$ | $0.73931 \times 10^{-2}$ | $0.10124 \times 10^{-1}$ | $0.86325 \times 10^{-2}$ | $0.86707 \times 10^{-2}$  | $0.949439 \times 10^{-2}$ |

(1.59 ppm of boron in the moderator)

- (1) Undepleted Fuel: 0.72% U-235      (2) Depleted Fuel: 0.52% U-235  
 (3) Reflector: 99.722% D<sub>2</sub>O

**Table 8. Axially Averaged Effective Two-Group Constants**

| Parameter         | Region                   | Outer Undepleted Fuel Zone | Inner Zone<br>(2 Depleted Fuel Bundles/Channel) |                             |
|-------------------|--------------------------|----------------------------|---|-----------------------------|
|                   |                          |                            | 8th & 9th Bundle<br>(set 1)                     | 6th & 7th Bundle<br>(set 2) |
|                   |                          |                            | $D_1$   | 1.3158                      |
| $D_2$             | 0.95769                  | 0.955775                   | 0.95769   |                             |
| $\Sigma_{a1}$     | $0.10042 \times 10^{-2}$ | $0.10071 \times 10^{-2}$   | $0.10071 \times 10^{-2}$                        |                             |
| $\Sigma_{a2}$     | $0.37554 \times 10^{-2}$ | $0.36702 \times 10^{-2}$   | $0.36436 \times 10^{-2}$                        |                             |
| $\nu \Sigma_{f2}$ | $0.44679 \times 10^{-2}$ | $0.42394 \times 10^{-2}$   | $0.41680 \times 10^{-2}$                        |                             |
| $\Sigma_{r1}$     | $0.86329 \times 10^{-2}$ | $0.86798 \times 10^{-2}$   | $0.86789 \times 10^{-2}$                        |                             |

and partly due to the decrease in moderator density. The net effect on infinite multiplication factor is negative as shown in Fig. 6. Addition of boron into moderator results in further reduction in cell multiplication. The variation of cell multiplication as the boron poison concentration is varied is drawn in Fig. 7.

Effect of coolant temperature changes on  $k_{\infty}$  is next considered. An increase in coolant temperature results in a decrease in coolant density. This then gives rise to a net increase in  $k_{\infty}$  due to an increase in fast fissions and a decrease in resonance absorption. Fig. 8 shows the variation of cell reactivity versus the coolant temperature changes around its nominal operational value.

Upon comparison of LATREP results with PSR values we observe both reasonable agree-

ments and some discrepancies. Let's take Table 2, for instance. LATREP predicts the lattice cell parameters which are in a fairly good agreement with PSR<sup>2)</sup> values. However, Fig. 5 shows that LATREP underestimates the burnup effects of fuel temperature coefficient compared with the PSR<sup>3)</sup> value. Though unclearified at the moment, this difference is supposedly due to the way the fuel composition at the specific burnup level is approximated. Apparently the PSR value is based on the fuel composition averaged over all the fuel bundle irradiations present in the core, while in LATREP computation the fuel composition is referred to that of a single fresh fuel bundle irradiation. One next point worthy to note is the coolant temperature coefficient. As shown in Fig. 8, LATREP predicts that an increase in

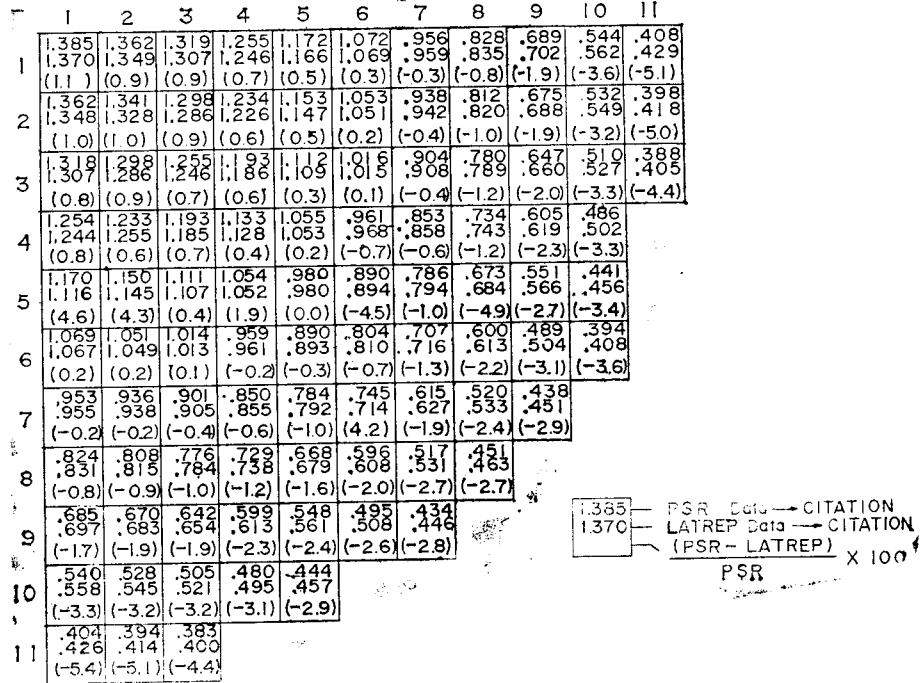


Fig. 9. Power Distribution for Core Plane(Undepleted Fuel Bundle Only)

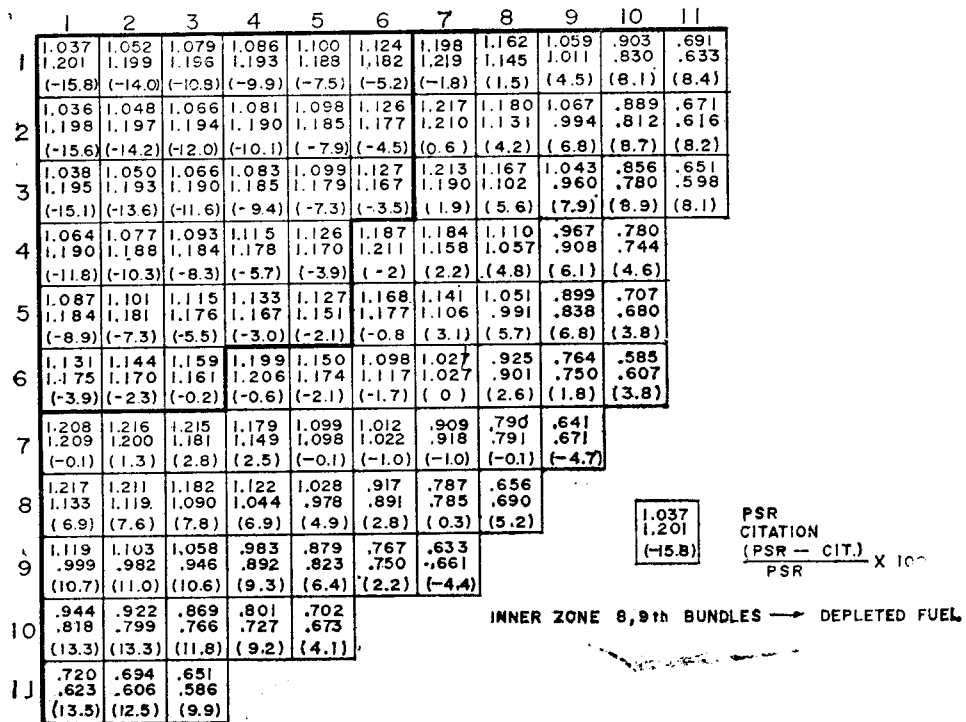


Fig. 10. Channel Power Distribution



|    | 1                        | 2                        | 3                        | 4                        | 5                        | 6                        | 7                        | 8                        | 9                       | 10                     | 11                    |
|----|--------------------------|--------------------------|--------------------------|--------------------------|--------------------------|--------------------------|--------------------------|--------------------------|-------------------------|------------------------|-----------------------|
| 1  | 1.037<br>1.042<br>(-0.5) | 1.052<br>1.047<br>(0.5)  | 1.079<br>1.057<br>(2.0)  | 1.086<br>1.073<br>(1.2)  | 1.100<br>1.094<br>(0.5)  | 1.124<br>1.121<br>(0.3)  | 1.198<br>1.211<br>(-1.2) | 1.162<br>1.167<br>(-0.4) | 1.059<br>1.050<br>(0.8) | .903<br>.871<br>(3.5)  | .691<br>.669<br>(3.2) |
| 2  | 1.036<br>1.046<br>(-1.0) | 1.048<br>1.051<br>(-0.3) | 1.066<br>1.061<br>(0.5)  | 1.081<br>1.076<br>(0.5)  | 1.098<br>1.097<br>(0.1)  | 1.126<br>1.121<br>(0.4)  | 1.217<br>1.206<br>(0.9)  | 1.180<br>1.156<br>(2.0)  | 1.067<br>1.034<br>(3.1) | .889<br>.835<br>(6.1)  | .671<br>.652<br>(2.8) |
| 3  | 1.038<br>1.055<br>(-1.6) | 1.050<br>1.060<br>(-1.0) | 1.066<br>1.069<br>(-0.3) | 1.083<br>1.086<br>(-0.3) | 1.099<br>1.103<br>(-0.4) | 1.127<br>1.122<br>(0.4)  | 1.213<br>1.196<br>(1.4)  | 1.167<br>1.131<br>(3.1)  | 1.043<br>1.001<br>(4.0) | .853<br>.821<br>(4.1)  | .651<br>.663<br>(2.1) |
| 4  | 1.064<br>1.069<br>(-0.5) | 1.077<br>1.073<br>(0.4)  | 1.093<br>1.082<br>(1.0)  | 1.115<br>1.095<br>(1.8)  | 1.126<br>1.111<br>(1.3)  | 1.187<br>1.200<br>(-1.1) | 1.184<br>1.175<br>(0.8)  | 1.110<br>1.092<br>(1.6)  | .967<br>.951<br>(1.7)   | .780<br>.785<br>(-0.6) |                       |
| 5  | 1.087<br>1.089<br>(-0.2) | 1.101<br>1.092<br>(0.8)  | 1.115<br>1.099<br>(1.4)  | 1.133<br>1.109<br>(2.1)  | 1.127<br>1.114<br>(1.2)  | 1.168<br>1.184<br>(-1.4) | 1.141<br>1.134<br>(0.6)  | 1.051<br>1.031<br>(1.9)  | .899<br>.880<br>(2.1)   | .707<br>.717<br>(-1.4) |                       |
| 6  | 1.131<br>1.113<br>(1.6)  | 1.144<br>1.113<br>(2.7)  | 1.159<br>1.116<br>(3.7)  | 1.199<br>1.194<br>(0.4)  | 1.150<br>1.180<br>(-2.6) | 1.098<br>1.141<br>(-3.9) | 1.027<br>1.042<br>(-1.5) | .927<br>.944<br>(-2.1)   | .764<br>.792<br>(-3.7)  | .585<br>.633<br>(-8.2) |                       |
| 7  | 1.208<br>1.201<br>(0.6)  | 1.216<br>1.193<br>(1.9)  | 1.215<br>1.184<br>(2.6)  | 1.179<br>1.165<br>(1.2)  | 1.099<br>1.125<br>(-2.4) | 1.012<br>1.031<br>(-1.9) | .909<br>.959<br>(-5.5)   | .790<br>.835<br>(-5.7)   | .641<br>.714<br>(-10.2) |                        |                       |
| 8  | 1.217<br>1.153<br>(5.3)  | 1.211<br>1.141<br>(5.8)  | 1.182<br>1.117<br>(5.5)  | 1.122<br>1.076<br>(4.1)  | 1.028<br>1.016<br>(1.2)  | .917<br>.931<br>(-1.5)   | .787<br>.826<br>(-5.0)   | .656<br>.727<br>(-10.8)  |                         |                        |                       |
| 9  | 1.119<br>1.035<br>(7.5)  | 1.103<br>1.018<br>(7.7)  | 1.058<br>.984<br>(7.0)   | .983<br>.932<br>(5.2)    | .879<br>.863<br>(5.2)    | .767<br>.790<br>(-1.8)   | .633<br>.698<br>(-3.0)   |                          |                         |                        |                       |
| 10 | .944<br>.857<br>(9.2)    | .922<br>.839<br>(9.9)    | .869<br>.803<br>(7.6)    | .801<br>.766<br>(4.4)    | .701<br>.710<br>(-1.1)   |                          |                          |                          |                         |                        |                       |
| 11 | .720<br>.657<br>(8.8)    | .694<br>.639<br>(7.9)    | .651<br>.614<br>(5.7)    |                          |                          |                          |                          |                          |                         |                        |                       |

1.037 → PSR  
 1.042 → CITATION  
 (-0.5) →  $\frac{(PSR - CIT.)}{PSR} \times 100$

INNER ZONE 6,7th BUNDLES → DEPLETED FUEL

Fig. 11. Channel Power Distribution

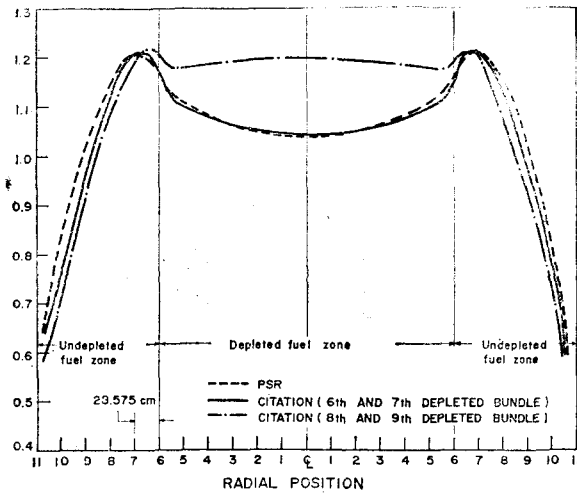


Fig. 12. Channel Power Distribution

coolant temperature gives rise to the increase in the cell multiplication, i.e., the positive coolant temperature coefficient. Since any change in power level directly influences the coolant

temperature via fuel temperature change, the positive reactivity effect of the coolant temperature on reactor stability should be investigated carefully. To our best knowledge, this point is not mentioned in the PSR<sup>33</sup> yet.

4.2. Two-Group Diffusion Theory Constants

The lattice cell parameters computed in the previous section can be utilized to generate the equivalent homogenized two-group diffusion theory parameters for core physics calculations. Table 6 tabulates the two-group constants of the unborated, undepleted fresh fuel channel with regard to four initial operating conditions specified in Table 3. The effects of boron addition into moderator on two-group constants are also evaluated for two fresh fuel channels, depleted and undepleted. Table 7 compares the PSR<sup>33</sup> value with LATREP output for two fuel channels in which boron is dissolved into moderator by 1.59 ppm in weight.

Two-group constants in Table 6 or 7, if used directly in 2-dimensional diffusion theory computation, may lower the accuracy in the core channel power distribution. This is because the real, 3-dimensional reactor core is non-uniform in the third dimension which is not treated in 2-dimensional computation. For the case of CANDU-PHWR core, each channel is considered axially non-uniform either for the mixed alignment of fuel bundles of different fissile contents or for non-uniform burnup and different axial leakage. In the face of this non-uniformity of the channel, the two-group constants are modified by means of the axially averaging code of group constants, HWRAXAV<sup>6)</sup>.

Listed in Table 8 are the effective two-group constants averaged along the axial direction in the spirit of HWRAXAV code. In treating core inner zone, we assumed two different channel configuration; one case that two depleted fuel bundles are located in the axial positions No. 8 and No. 9 and the other in axial positions No. 6 and No. 7. It is noted that LATREP predicts quite a different set of two-group constants from the PSR<sup>3)</sup>. This discrepancy, however, seems to be fortuitous in view of the facts that equivalent homogenized group constants are in general not unique and that they depend on the method employed for homogenization and group condensation.

#### 4.3. Channel Power Distribution

The computations of channel power distribution in the core are performed by introducing the effective two-group constants into the 2-dimensional diffusion equation code, CITATION<sup>7)</sup>.

The first step in computation is to assume the confidence in the accuracy of the LATREP-predicted cross section data. For this purpose X-Y power distributions calculated using LATREP-predicted two-group constants are compared with that obtained from PSR values. Fig. 9 shows that two sets of group constants

result in almost identical power distribution for core plane consisting solely of undepleted fuel bundles.

Fig. 10 and 11 represent the channel power distribution calculated using set (1) and set (2) two-group constants in Table 8. It is shown that set (2) two-group cross sections give the channel power distribution in a better agreement with PSR<sup>3)</sup> than set (1) data. This is more obvious when the channel power distribution is viewed along a radial direction, as depicted in Fig. 12.

#### 5. Conclusion

The numerical results presented in this paper on lattice properties and core channel power distributions of Wolsung PHWR core are of a preliminary nature. This is so partly because the 3-dimensional Wolsung core is approximately represented by a 2-dimensional one and partly because the presence of adjuster rods and zone control systems that provide the control absorber to shape the spatial power distribution is not taken into account in the 2-dimensional CITATION computation.

The combination of LATREP/CITATION computer codes with regard to the core physics analysis of Wolsung PHWR appears to be satisfactory in the sense that they reproduce most of the lattice cell and core design parameters within an acceptable error bound. However, the discrepancies that we mentioned in Section 4 make it necessary a further investigation before the use of these codes is justified. In this regard it is considered that the exact core configuration of the Wolsung PHWR must be known prior to any future attempt to improve our computation.

Finally, the positive reactivity effects of coolant temperature supposedly plays an important role in analyzing the stability characteri-

stics of the Wolsung core. Though it may not be a critical factor to determine the safety of the reactor, the effect should be carefully discussed in any future issue of the Safety Analysis Report of the Wolsung PHWR.

#### **Acknowledgement**

This work is supported by the Asan Foundation, which granted a research fund to two of the authors (Chang Hyun Chung and C.H. Kim). The computation was carried out at the Computer Center of the Korea Institute of Science and Technology.

#### **References**

1. 2×600 MWe CANDU-PHW Nuclear Generating Station for the KECO, Preliminary Safety Analysis Report; Vol. 2, Jan. 1974.
2. 600 MWe CANDU-PHW Wolsung-1 Nuclear Generating Station for the KECO, Preliminary Safety Report; Vol. 2, Feb. 1976.
3. 600 MWe CANDU-PHW Wolsung-1 Nuclear Generating Station for the KECO, Safety Report; Vol. 1, June 1977.
4. G.J. Phillips and J. Griffiths, "LATREP User's Manual", AECL-3857 (1971).
5. Gibson, I.H., "The Physics of LATREP", AECL-2548 (1966).
6. HWRAXAV: HWR Axial Averaging Code; Nuclear Design Section, KAERI.
7. T.B. Fowler, D.R. Vondy and G.W. Cunningham, Nuclear Reactor Core Analysis Code: CITATION, ORNL-TM-2496, Rev. 2.
8. J. Griffiths, The Effectiveness of LATREP Calculation; A Survey and Detailed Comparison with Experiment, AECL-3739 (1971).